Available online at www.sciencedirect.com
ScienceDirect
Journal of Pharmaceutical and Biomedical Analysis 43 (2007) 1306–1314
JOURNAL OF PHARMACEUTICAL AND BIOMEDICAL ANALYSIS
www.elsevier.com/locate/jpba

Complete resolution of the microscopic protonation equilibria of *N*-methyl-D-aspartic acid and related compounds

Miklós Boros [a,*], József Kökösi [a], József Vámos [a], Béla Noszál [a,b]

[a] *Semmelweis University, Department of Pharmaceutical Chemistry, Hőgyes E. u. 9, Budapest 1092, Hungary*
[b] *Hungarian Academy of Sciences, Semmelweis University, Research Group for Drugs of Abuse and Doping Agents, Hőgyes E. u. 9, Budapest 1092, Hungary*

Received 22 August 2006; received in revised form 1 October 2006; accepted 24 October 2006
Available online 11 December 2006

Abstract

Protonation equilibria of *N*-methyl-D-aspartate (NMDA, a specific glutamate receptor agonist) and its derivatives are characterized at the macroscopic and microscopic levels. ^{1}H NMR–pH and pH-potentiometric titrations were carried out to determine the macroconstants. Microconstants were obtained by appropriate combination of acidity and NMR parameters of the parent compound and its three synthetic derivatives. These derivatives were close models of the NMDA minor microspecies, allowing the calculation of all the 12 microconstants, the 8 microspecies concentrations and 3 site interactivity parameters. Reliability of the microconstants was assessed by three independent test methods. It was found that protonation of the secondary amino site decreases the β- and α-carboxylate basicities almost exactly by one and two orders of magnitude, respectively, whereas protonation of one of the carboxylates lessens the basicity of the other one by a factor of 3. NMR–pH profiles, macro- and microscopic protonation schemes and species-specific distribution diagrams are presented.

Keywords: NMDA; ^{1}H NMR–pH titration; pH-potentiometric titration; Microconstant; Microspecies; Basicity; pH-dependent distribution; Pair interactivity

1. Introduction

Acidity of the terminal groups in glutamate receptor agonists has been found to influence the degree of receptor activation [1]. In fact, a relationship has been reported between the ionization constants of ω-carboxylic groups and receptor-binding capacity [2]. The site-specific acid–base properties of glutamate, AMPA, NMDA and other glutamate receptor ligands are therefore of fundamental importance to understand, quantitate and modulate ligand–receptor interactions at the molecular level. Also, these parameters allow to design and develop selective analytical methods, especially in capillary electrophoresis.

N-Methyl-D-aspartate (NMDA) has been identified as one of the few endogenous, subtype-selective glutamate receptor agonists in mammalian central nervous systems [3]. NMDA receptors are important in memory formation, synaptic plasticity [4], whereas their malfunctions (mostly over-excitation) are related to barely curable neurodegenerative disorders [5,6] such as Huntington's disease [7], CNS ischemia [8], schizophrenia [9,10] and Alzheimer's disease [11].

The biological versatility of NMDA and other endogenous neurotransmitters stems from their flexibility in charge, charge-distribution and conformation [12–14], which makes the adaptability of these small molecules so that they can take up different forms at receptor surfaces and membranes. Although a large number of NMDA agonists and antagonists have been synthesized and reported [15,16], the site-specific acid–base properties, a fundamental element to explore the (patho)biochemical behavior of these compounds have not yet appeared. The lack of such data lies in the trifunctional nature, the proximity of sites, the compact electronic system of NMDA and the concomitant difficulties in the thorough characterization.

NMDA has a four-carbon backbone with three ionizable moieties that effect the electron density of every atom in the molecule to a certain, unknown extent. Thus, none of the chemical shift changes of any adjacent NMR nuclei reflect selectively the protonation state of any individual

* Corresponding author. Tel.: +36 1 431 4348.
E-mail address: bormik@mail.tvnet.hu (M. Boros).

0731-7085/$ – see front matter © 2006 Elsevier B.V. All rights reserved.
doi:10.1016/j.jpba.2006.10.040

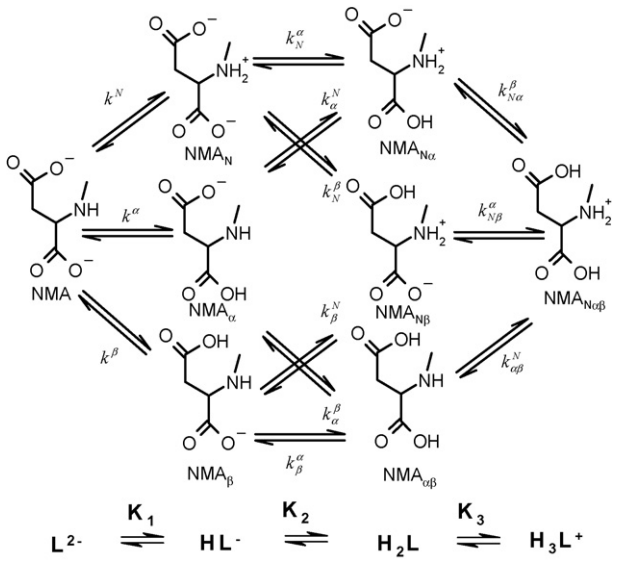

Scheme 1. Macroscopic and microscopic protonation scheme of NMA.

sites. Consequently, no direct spectroscopic or other measurement can monitor the pH-dependent state of the functional groups in NMDA. Quantitation of intrinsic basicities therefore inevitably needs data from analogous moieties in auxiliary compounds.

Here we report the acid–base properties of the title compound and its three amide derivatives at the molecular and submolecular levels, studied by pH-potentiometric and NMR–pH titrations, using acidity and NMR-based evaluations. The amides serve as models of some of the NMDA microspecies with reduced acid–base complexity. Since acid–base titrations under achiral circumstances are not based on stereo-specific reactions, the racemic forms of compounds, i.e. *N*-methyl-DL-aspartic acid (NMA, 2-methylamino-succinic acid **1**), NMA-α-amide (NMAαa, 3-methylamino-succinamic acid **2**), NMA-β-amide (NMAβa, 2-methylamino-succinamic acid **3**) and NMA-diamide (NMAαβa, 2-methylamino-succinamide **4**; Schemes 1 and 2) were used.

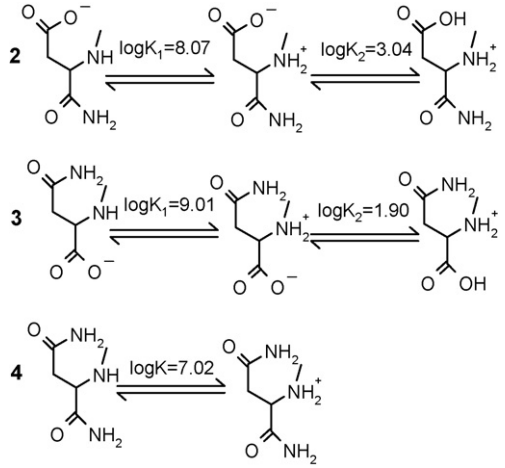

Scheme 2. Protonation equilibria of NMA amide derivatives.

2. Experimental

2.1. Materials

NMA (analytical grade) was purchased from Sigma and was used without further purification. Other reagents were also of analytical grade. Synthesis of NMA-α-amide, NMA-β-amide and NMA-diamide will be reported elsewhere. All solutions were prepared from bidistilled Millipore water.

2.2. Potentiometric titrations

Potentiometric titrations were performed at $25.0 \pm 0.1\,^{\circ}C$ and 0.15 M ionic strength, adjusted with NaCl. A Metrohm 716 DMS Titrino autoburet (Metrohm, Switzerland) equipped with a Metrohm 6.0238.000 combined glass electrode was used. The electrode system was calibrated in terms of hydrogen ion concentration [17,18] by titrating 5 ml of 0.05 M HCl with standardized 0.05 M NaOH. Both stock solutions contained calculated amounts of NaCl to ensure the 0.15 M constant ionic strength. For protonation constant determinations, a weighed amount of the ligand was dissolved in the HCl stock solution and titrated with NaOH. Measurements of **1** and **3** were performed at 0.01 M ligand concentration. All concentration-based protonation macroconstants were evaluated by the nonlinear least-squares regression program PROTC [19].

2.3. ^{1}H NMR titrations with in situ pH monitoring

To determine the corresponding pH of each ^{1}H NMR spectra, electrodeless single tube NMR titration method was applied [20] with indicator molecules: dichloroacetic acid ($\log K = 1.14$, $\delta_{Ind} = 6.055$, $\delta_{HInd} = 6.345$), chloroacetic acid ($\log K = 2.70$, $\delta_{Ind} = 4.049$, $\delta_{HInd} = 4.280$), acetic acid ($\log K = 4.51$, $\delta_{Ind} = 1.907$, $\delta_{HInd} = 2.086$), 1H-imidazole [21] ($\log K = 7.08$, $\delta_{IndH2} = 7.765$, $\delta_{HInd} = 8.672$, $\delta_{IndH4} = 7.128$ $\delta_{HIndH4} = 7.472$) and tris(hydroxymethyl)-aminomethane [TRIS] ($\log K = 8.13$, $\delta_{Ind} = 3.509$, $\delta_{HInd} = 3.733$). In strongly basic media ($9 < pH < 11$), trimethyl-amine hydrochloride ($\log K = 9.91$, $\delta_{Ind} = 2.168$, $\delta_{HInd} = 2.904$) was introduced. Advantages of trimethylamine as pH-indicator are the large difference between limiting chemical shifts ($\Delta\delta = 0.736$ ppm) that improves the accuracy of measurements, and a singlet signal of nine equivalent hydrogens allowing to keep concentration of trimethylamine at 0.5 mM. The protonation constant of trimethylamine was determined by differential potentiometric titration.

0.6 ml solutions were prepared for NMR titrations, each contained 0.5 mM sodium 3-(trimethylsilyl)-1-propanesulfonate (DSS) as internal chemical shift reference (chemical shift of DSS is insensitive to the solution pH [22]), 0.1–0.14 M NaCl to give ionic strength of 0.15 M, and 0.02 M of the ligands (**1**, **2**, **3**, **4**). In cases of all the compounds, the acidic and basic intervals of titrations have been carried out separately, due to stability problems and to improve reproducibility.

All solutions contained additional indicator molecules and pH adjusting acids or bases as follows:

Compound **1** (acidic part): 4 mM dichloroacetic acid, 2 mM chloroacetic acid, 1 mM acetic acid, 1 mM TRIS as indicators, 0.026 M NaOH to set the starting pH to 6.65.

Compound **1** (basic part): 1 mM acetic acid, 1 mM TRIS, 0.5 mM trimethyl-amine hydrochloride as indicators, 0.01 M NaOH to set the starting pH to 6.58.

Compound **2** (acidic part): 2 mM chloroacetic acid, 1 mM acetic acid, 1 mM TRIS as indicators and 0.01 M NaOH to set the starting pH to 6.51.

Compound **2** (basic part): 1 mM acetic acid, 1 mM TRIS, 0.5 mM trimethyl-amine hydrochloride as indicators, starting pH was 5.07.

Compound **3** (acidic part): 4 mM dichloroacetic acid, 2 mM chloroacetic acid, 1 mM acetic acid, 1 mM TRIS as indicators, 0.01 M NaOH to set the starting pH to 7.72.

Compound **4** (basic part): 1 mM acetic acid, 1 mM TRIS, 0.5 mM trimethyl-amine hydrochloride, 4 mM ^{1}H-imidazole as indicators, 0.013 M HCl to set the starting pH to 6.57.

Titrants were 0.005–0.15 M NaOH or 0.005–0.15 M HCl, and were added with a fine syringe in 3–20 μl portions after the previous spectrum was registered. The contents of the NMR tube were homogenized, and a new spectrum was recorded. Titrants also contained 0–0.14 M NaCl for ionic strength adjustment, and 0.02 M of the assayed compounds **1**–**4** to avoid dilution.

Titrations of compounds **1**–**3** were carried out on 500 MHz, whereas compound **4** was titrated on 600 MHz Varian Inova Unity spectrometers. All solutions contained 3% D_2O by volume, this deuterium concentration proved to be enough for the spectrometer lock system. ^{1}H NMR spectra were recorded at 25 °C, and the resonance of solvent H_2O was diminished by a selective presaturation pulse before the observation pulse.

The corresponding pH of each NMR spectrum was determined from the actual chemical shift of the appropriate indicator molecule [20]. The NMR–pH datasets were fitted with Statistica 6.0 [23], nonlinear estimations/user specified regression module, to determine protonation macroconstants from individual carbon-bound hydrogen chemical shift-connected pH pairs. Multiple fitting was performed with Origin 7 SR2 [24].

3. Results and discussion

N-Methyl-aspartate, a dianionic species (L^{2-}) carries three basic sites: an α-*N*-methyl-amino (N), an α-, and a β-carboxylate group. Its protonation equilibria are symbolized as follows:

$$L^{2-} \overset{K_1}{\rightleftharpoons} HL^- \overset{K_2}{\rightleftharpoons} H_2L \overset{K_3}{\rightleftharpoons} H_3L^+ \quad (1)$$

where K_1, K_2, K_3, the stepwise (successive) protonation macroconstants quantitate the association of hydrogen ions.

A recently developed electrodeless, "single tube" NMR titration method of Szakács et al. [20] was primarily used for macroconstant evaluations, applying the reported in-tube indicator molecules, and introducing trimethyl-amine as new indicator molecule in basic media.

4. Evaluation of the macroconstants

Evaluation of the macroconstants from ^{1}H NMR–pH titration curves applied the principle that nonexchanging NMR nuclei in the vicinity of the basic site sense different electronic environments upon protonation [25]. The observed carbon-bound hydrogens were the *N*-methyl singlet, and the 12-peak ABX pattern of the methylene and methyne hydrogens. Chemical sifts were obtained by second order analyses of spectra [26]. Scalar couplings of the ABX system were also calculated and will be applied for conformational analyses in another study. Since protonation processes are instantaneous on the NMR chemical shift time scale, the observed chemical shift of a certain nucleus (Table 1) can be expressed as a weighted average of chemical shifts of the mono-, di-, and triprotonated forms of NMA.

$$\delta^{obs} = \delta_{L^{2-}} f_{L^{2-}} + \delta_{HL^-} f_{HL^-} + \delta_{H_2L} f_{H_2L} + \delta_{H_3L^+} f_{H_3L^+} \quad (2)$$

Weighting factors are mole fractions that can be expressed in terms of stepwise protonation macroconstants of **1** and the actual hydrogen ion concentration. For example, f_{H_2L} is

$$f_{H_2L} = \frac{[H_2L]}{[L^{2-}] + [HL^-] + [H_2L] + [H_3L^+]} = \frac{K_1K_2[H^+]^2}{1 + K_1[H^+] + K_1K_2[H^+]^2 + K_1K_2K_3[H^+]^3} \quad (3)$$

Combining and rearranging Eqs. (2) and (3) yielded Eq. (4) that can be directly fitted to the ^{1}H NMR titration curve of each nucleus observed.

$$\delta^{obs} = \frac{\delta_{L^{2-}} + \delta_{HL^-} K_1[H^+] + \delta_{H_2L} K_1K_2[H^+]^2 + \delta_{H_3L^+} K_1K_2K_3[H^+]^3}{1 + K_1[H^+] + K_1K_2[H^+]^2 + K_1K_2K_3[H^+]^3} \quad (4)$$

Since symbols L^{2-}, HL^- and H_3L^+ stand for predominant macrospecies in basic, neutral and highly acidic pH ranges, respectively, the corresponding chemical shifts $\delta_{L^{2-}}$, δ_{HL^-} and $\delta_{H_3L^+}$ can be directly read from the NMR spectra of appropriate pH (Table 1).

In contrast, the formation of macrospecies H_2L overlaps with that of H_3L^+, showing no plateau in the titration curve, covering protonation of both the β- and α-carboxylates, and the two isomeric, coexisting species, $NMA_{N\beta}$ and $NMA_{N\beta}$ (Scheme 1). The δ_{H_2L} value of each nucleus has therefore been obtained from fitting Eq. (4) to the corresponding ^{1}H NMR titration curve, and was calculated by introducing $\log K_2 = 3.54$ (determined by pH-potentiometry, see later) of NMA as a constant value.

Chemical shifts of *N*-methyl, methylene and methyne carbon-bound hydrogens are shown as a function of pH in Fig. 1.

Table 1
^{1}H NMR chemical shifts of NMA macrospecies

	X	A	B	N-Me	Observation pH
$\delta_{L^{2-}}$ (ppm)	3.281	2.487	2.281	2.253	13
δ_{HL^-} (ppm)	3.733	2.811	2.701	2.746	7
δ_{H_2L} (ppm)	3.989	3.061	3.055	2.776	
$\delta_{H_3L^+}$ (ppm)	4.314	3.241	3.202	2.846	1

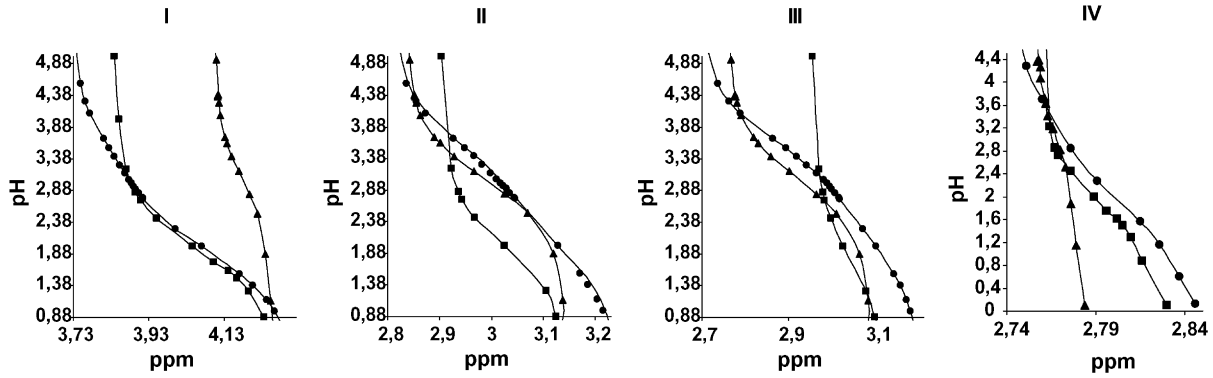

Fig. 1. Protonation shifts of methyne (I), methylene A (II), methylene B (III), and *N*-methyl hydrogens (IV) in NMA (●), α- (▲) and β- (■) amides in acidic pH ranges. Computer fits are shown in solid lines.

Titration curves prove that all the four chemical shifts are significantly influenced by the protonation state of all three acid–base functional groups, including even the *N*-methyl group, the chemical shift of which shows some change in the acidic region.

Differential pH-potentiometric titrations were performed for three reasons: to prove the lack of possible disturbing interactions in the NMR tube between the substances studied and the indicator molecules, to obtain or control the K_1 and K_2 values of **1** and K_1 value of **3**, and also to prove that 3% D_2O in the ^1H NMR solutions has negligible solvent isotope effect on the $\log K$ values [19].

Potentiometric titration curves were transformed into Bjerrum plots (Eq. (5) and Fig. 2), which show the mean number of protons $\bar{n}_H$ associated with one ligand molecule at any pH [27].

$$\bar{n}_H = \frac{[HL^-] + 2[H_2L] + 3[H_3L^+]}{[L^{2-}] + [HL^-] + [H_2L] + [H_3L^+]} = \frac{K_1[H^+] + 2K_1K_2[H^+]^2 + 3K_1K_2K_3[H^+]^3}{1 + K_1[H^+] + K_1K_2[H^+]^2 + K_1K_2K_3[H^+]^3} \quad (5)$$

Macroconstants obtained by NMR–pH and pH-potentiometric titrations are shown in Scheme 2 and Table 4. All values are in agreement with chemical evidence. Due to the improved precision and accuracy of the reported [20] electrodeless ^1H NMR–pH titration method at pH < 2, the $\log K_3 = 1.85$ value was accepted for NMA. $\log K_2 = 3.54$ has been introduced from the pH-potentiometric titration, and was kept constant in the NMR–pH fitting, to avoid ambiguity that lies in the simultaneous chemical shift and protonation constant parameter estimations when none of the values is known a priori (δ_{H_2L} and $\log K_2$ in this case). Potentiometric titrations and the subsequent Bjerrum analyses do not suffer from such a problem, therefore $\log K_2 = 3.54$ was accepted and employed in microconstant calculations. The agreement of K_1 values of compounds **1** and **3** measured by pH-potentiometriy and NMR–pH titrations provide evidence that no tangible interactions occur between substances in the NMR tube.

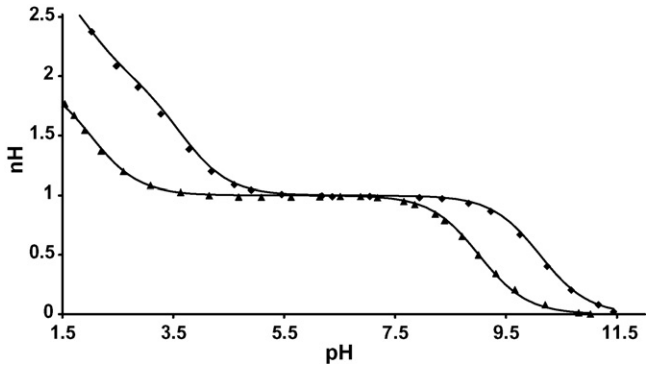

Fig. 2. Bjerrum plots from the potentiometric titrations of NMA (♦) and NMA-β-amide (▲). Computer fits are shown in solid lines.

Two, well-separated pH ranges of protonation processes occur on the NMA and NMA-β-amide titration curves (Fig. 2), allowing division of the complete titration curve into a monoprotic and a diprotic one for NMA. In basic pH regions the regular sigmoidal shape, typical of monoprotic systems, indicates that $\log K_1$ can overwhelmingly be assigned to the methylamino group in each compound. Protonations between pH 7 and pH 0 take place in an overlapping fashion for NMA, covering the α-, and β-carboxylate associations with hydrogen ions.

5. The microequilibrium analysis of NMA

Microequilibria, in general, are analyzed either when sites of comparable basicity bind the proton, producing microspecies of commeasurable concentration, or in cases when concentrations are very different, but the minor microspecies can be the reactive one [14,28]. NMA has both capacities, therefore its full microequilibrium analysis is considered here.

Scheme 1 depicts the complete microequilibrium scheme of NMA, with 8 microspecies and 12 microconstants. The corresponding macroscopic species and constants are also shown.

Protonation microconstants k^N, k^α, k^β, k^α_N, k^β_N, k^N_α, k^β_α, etc., on the double arrows are, by definition, specific basicity parameters of a particular molecular subunit, in a defined protonation state for the rest of the molecule. For instance, $k^\beta_{N,\alpha}$ can be expressed as

$$k^\beta_{N,\alpha} = \frac{[NMA_{N\alpha\beta}]}{[NMA_{N\alpha}][H^+]} \quad (6)$$

The subscript of microconstants and microspecies indicates the group(s) already protonated, whereas the superscript of microconstants k labels the actual site of protonation equilibrium in question. The relationships between macro- and microconstants are as follows:

$$K_1 = k^{\mathrm{N}} + k^{\beta} + k^{\alpha} \tag{7}$$

$$K_1K_2 = k^{\mathrm{N}}k^{\beta}_{\mathrm{N}} + k^{\mathrm{N}}k^{\alpha}_{\mathrm{N}} + k^{\beta}k^{\alpha}_{\beta} = k^{\beta}k^{\mathrm{N}}_{\beta} + k^{\alpha}k^{\mathrm{N}}_{\alpha} + k^{\alpha}k^{\beta}_{\alpha} \tag{8}$$

$$K_1K_2K_3 = k^{\mathrm{N}}k^{\beta}_{\mathrm{N}}k^{\alpha}_{\mathrm{N},\beta} = k^{\mathrm{N}}k^{\alpha}_{\mathrm{N}}k^{\beta}_{\mathrm{N},\alpha} = k^{\beta}k^{\mathrm{N}}_{\beta}k^{\alpha}_{\mathrm{N},\beta} = k^{\beta}k^{\alpha}_{\beta}k^{\mathrm{N}}_{\alpha,\beta} = k^{\alpha}k^{\mathrm{N}}_{\alpha}k^{\beta}_{\mathrm{N},\alpha} = k^{\alpha}k^{\beta}_{\alpha}k^{\mathrm{N}}_{\alpha,\beta} \tag{9}$$

Microspecies NMA_N, NMA_α, NMA_β, as well as $NMA_{N\alpha}$, $NMA_{N\beta}$ and $NMA_{\alpha\beta}$ are of the same stoichiometry, but they have different constitutions, due to different proton binding sites. The concentration ratio of these protonation isomers is independent of both the total concentration and pH, but it changes with ionic strength, temperature and other conditions that modify the thermodynamic stability. Since protonation reactions are instantaneous ones, microspecies cannot be separated by any experimental techniques, and microspecies-specific NMR chemical shifts cannot be determined directly. Rather, at least one external information is required [28].

Chemical evidences and ^{1}H NMR protonation shifts indicate that the major protonation pathway includes the NMA, NMA_N, $NMA_{N\beta}$ and $NMA_{N\alpha\beta}$ species and the k^{N}, k^{β}_{N} and $k^{\alpha}_{\mathrm{N},\beta}$ microconstants. The $\log K_2$ values of 2 and 3 (Scheme 2) and their comparison also provide evidence of this statement. $NMA_{N\alpha}$ is a commeasurable minor isomer of $NMA_{N\beta}$, whereas NMA_β, NMA_α and especially $NMA_{\alpha\beta}$ are the most minor species, the formation of which do not affect any spectra beyond the experimental error. Parameters of the latter three microspecies can therefore be elucidated from data of model compounds only, while those of $NMA_{N\alpha}$ can be obtained by exploiting both NMR–pH and acidity measurements.

Model compounds can mimic the behavior of minor protonation isomers well. For NMA this means, e.g. that an appropriate model embodies a microspecies in which a less-basic site (such as the α-carboxylate) is kept in its quasi-protonated form, while the more basic site(s) (such as the methylamino, or the β-carboxylate, or both) bind(s) the proton. The moiety that has traditionally been regarded and treated as quasi-protonated carboxylate ("frozen –COOH" in its inductive effects) is the carboxylic methyl ester, since Ebert's classical work [30]. It has been shown more recently, however, that the isoelectronic, and nearly bio-isosteric $-CONH_2$ is an even closer model of –COOH, especially in its inductive effects [14,29].

Thus, NMAαa **2**, NMAβa **3** and NMAαβa **4** are in acid–base properties the possibly closest models of microspecies NMA_β, NMA_α and $NMA_{\alpha\beta}$, respectively. Accordingly, using the macroconstants of the three amides (Scheme 2), the microequilibria of **2** and **3** can be quantitated, as shown in Table 2.

Table 2 shows two site-specific basicities for each moiety in the two monoamides. The larger and smaller values in each cell refer to the basicity of the site in question when the other site is unprotonated and protonated, respectively. Pair interactivity parameter (E, $\log E$) quantitates that protonation of either site decreases the basicity of the other site by 1.99 log units in NMAβa, and by 1.05 log units in NMAαa. Taking into account the four independently observed amino basicities (in log units: 10.06 NMA, 9.01 NMAβa, 8.07 NMAαa and 7.02 NMAαβa), a surprisingly perfect additivity of the α- and β-amidation effects occur. This indicates either that amides are excellent models of –COOH groups in their inductive effects, or that the α- and β-carboxylic groups exert their effect on the methylamino site as a bilateral interaction, i.e. independently from the rest of the molecule. Interactivity parameters are therefore the most uninfluenced ones by the rest of the molecule, and can be transplanted with high level of certainty into more complex systems such as NMA.

Table 2
Site-specific basicities and interactivity parameters of NMA-monoamides in logarithmic units

Parameter type	Parameter value in log k units	
	NMAαa	NMAβa
Methylamino basicity	8.07 7.02	9.01 7.02
α-Carboxylate basicity		3.89 1.90
β-Carboxylate basicity	4.09 3.04	
Interactivity ($\log E$)	1.05	1.99

6. Microspeciation in the NMA, NMA_N, $NMA_{N\beta}$ $NMA_{N\alpha}$ $NMA_{N\alpha\beta}$ cycle. Elucidation of the commensurable microconstants

Since the methylamino protonation takes place predominantly separately from that of the carboxylates (see the virtually horizontal line near pH 6 in the Bjerrum plot; Fig. 2), the NMA macroconstants K_2 and K_3 refer overwhelmingly to carboxylate protonations. Also, since $NMA_{\alpha\beta}$ is the most minor microspecies (the protonation constant of which can only be elucidated deductively from the diamide derivative), macroconstants K_2 and K_3 should be decomposed into microconstants k^{α}_{N}, k^{β}_{N}, $k^{\beta}_{\mathrm{N},\alpha}$ and $k^{\alpha}_{\mathrm{N},\beta}$ (Scheme 1). It can be stated qualitatively that the inductive effect of the methylammonium group causes the α-carboxylate group to be a weaker base than β, a chemical evidence analogous with aspartic acid [29].

Taking into consideration that $k^{\alpha} \lll k^{\beta}k^{\mathrm{N}}$ and $k^{\beta}k^{\alpha}_{\beta}k^{\mathrm{N}}k^{\alpha}_{\mathrm{N}} \lll k^{\mathrm{N}}k^{\beta}_{\mathrm{N}}$, Eqs. (7)–(9) can be simplified for calculation purposes as follows:

$$K_2 = k^{\beta}_{\mathrm{N}} + k^{\alpha}_{\mathrm{N}} \tag{10}$$

$$K_2K_3 = k^{\beta}_{\mathrm{N}}k^{\alpha}_{\mathrm{N},\beta} = k^{\alpha}_{\mathrm{N}}k^{\beta}_{\mathrm{N},\alpha} \tag{11}$$

Eqs. (10) and (11) are well-known four microspecies formulas, where K_2 and K_3 are known quantities, and one extra piece of information is needed to elucidate the respective microconstants. Such extra information can be the microconstant

of one of the protonation isomers (preferably the minor one), site-specific protonation mole fractions, or the interactivity parameter, imported from an analogous moiety of a close derivative. Here we introduced the log K_2 value of NMAαa as $k^{\beta}_{N,\alpha}$, a microconstant of the minor protonation isomer. In order to verify this introduction, we applied three tests:

- log K_2 of NMAβa as control of the calculated $k^{\alpha}_{N,\beta}$;
- logk^{α}_{N} from normalized Sudmeier–Reilley ^{1}H NMR–pH equations;
- comparison of the interactivity parameter with the corresponding aspartic acid data [29].

The log K_2 value of NMAαa is 3.04, the introduction of which into $k^{\beta}_{N,\alpha}$ of Eqs. (10) and (11) results in the following constants: log$k^{\alpha}_{N} = 2.35$, log$k^{\beta}_{N} = 3.51$ and log$k^{\alpha}_{N,\beta} = 1.88$. The log K_2 value of NMAβa is 1.90, in excellent agreement with the calculated log$k^{\alpha}_{N,\beta} = 1.88$ value. As a second control, the Sudmeier–Reilley approach was used, based on the following principles.

The chemical shifts of the methylene and methyne hydrogens of NMA in acidic region are influenced by the protonation state (f) of the alpha (α) and beta (β) carboxylate groups [31]. The observed protonation shift of a nucleus ($\Delta\delta_{pH}$) is the weighted sum of the protonation shift coefficient (C) of the basic sites, where weighting factors are the protonation mole fractions. Applying for NMR nucleus X, and carboxylates α and β, it yields:

$$\Delta\delta_{(pH)X} = f_{(pH)\alpha}C_{\alpha X} + f_{(pH)\beta}C_{\beta X} \quad (12)$$

where protonation mole fractions $f_{(pH)\alpha}$ and $f_{(pH)\beta}$ can be expressed in terms of microspecies concentrations and can then be transferred into micro- and macroconstants and hydrogen ion concentrations:

$$f_{(pH)\alpha} = \frac{[NMA_{N\alpha}] + [NMA_{N\alpha\beta}]}{[NMA_N] + [NMA_{N\beta}] + [NMA_{N\alpha}] + [NMA_{N\alpha\beta}]} = \frac{k^{\alpha}_{N}[H^+] + k^{\alpha}_{N}k^{\beta}_{N,\alpha}[H^+]^2}{1 + k^{\beta}_{N}[H^+] + k^{\alpha}_{N}[H^+] + k^{\beta}_{N}k^{\alpha}_{N,\beta}[H^+]^2} \quad (13)$$

$$f_{(pH)\beta} = \frac{[NMA_{N\beta}] + [NMA_{N\alpha\beta}]}{[NMA_N] + [NMA_{N\beta}] + [NMA_{N\alpha}] + [NMA_{N\alpha\beta}]} = \frac{k^{\beta}_{N}[H^+] + k^{\beta}_{N}k^{\alpha}_{N,\beta}[H^+]^2}{1 + k^{\beta}_{N}[H^+] + k^{\alpha}_{N}[H^+] + k^{\beta}_{N}k^{\alpha}_{N,\beta}[H^+]^2} \quad (14)$$

Introducing Eqs. (10) and (11), we obtain:

$$f_{(pH)\alpha} = \frac{k^{\alpha}_{N}[H^+] + K_2K_3[H^+]^2}{1 + K_2[H^+] + K_2K_3[H^+]^2} \quad (15)$$

$$f_{(pH)\beta} = \frac{(K_2 - k^{\alpha}_{N})[H^+] + K_2K_3[H^+]^2}{1 + K_2[H^+] + K_2K_3[H^+]^2} \quad (16)$$

Unifying Eqs. (12), (15) and (16) yields:

$$\Delta\delta_{(pH)X} = \frac{k^{\alpha}_{N}[H^+] + K_2K_3[H^+]^2}{1 + K_2[H^+] + K_2K_3[H^+]^2}C_{\alpha X} + \frac{(K_2 - k^{\alpha}_{N})[H^+] + K_2K_3[H^+]^2}{1 + K_2[H^+] + K_2K_3[H^+]^2}C_{\beta X} \quad (17)$$

Thus, the knowledge of four constants (macroconstants K_2 and K_3, and protonation shift coefficients $C_{\alpha X}$ and $C_{\beta X}$) allows the calculation of k^{α}_{N}, the single unknown quantity, by fitting Eq. (17) to the experimental data pairs $\Delta\delta_{(pH)X}$ and [H$^+$]. The values of $C_{\alpha X}$ and $C_{\beta X}$ are, however, not a priori known. These two unknown parameters and k^{α}_{N} are highly correlated and cannot be simultaneously obtained by direct fitting [32–34] of Eq. (17). Their sum can be obtained if complete protonation at both sites takes place ($f_{(pH)\alpha} = f_{(pH)\beta} = 1$), i.e. $\Delta\delta_{(pH)X}$ covers a sufficiently wide pH range:

$$\Delta\delta_{(pH)X} = C_{\alpha X} + C_{\beta X} = \Delta\delta_{(pH)X\,max} \quad (18)$$

Decomposing $\Delta\delta_{(pH)X\,max}$ into $C_{\alpha X}$ and $C_{\beta X}$ can be done for NMA by using NMAαa and NMAβa protonation shifts at the X, and also for the A and B nuclei.

Protonation shifts of these monoamides in the neutral–acidic pH range cover the effect of single carboxylate protonations (Fig. 1). The single-site maximum protonation shifts observed in the monoamides can be added up, and the sum can be matched to the corresponding $\Delta\delta_{(pH)max}$ value of NMA. Table 3 shows that nearly perfect additivity is the case for H_X (0.5 % deviation), while large deviations (27 and 16%) occur for H_A and H_B, respectively. Protonation shifts of such geminal nuclei are often prone to conformational changes [35,36], and they have been therefore ignored from further evaluation processes.

The normalized value for $C_{\alpha X}$ was obtained as follows:

$$C_{\alpha X} = \frac{\Delta\delta_{X\,max,NMA}}{\Delta\delta_{X\,max,NMA\alpha a} + \Delta\delta_{X\,max,NMA\beta a}}\Delta\delta_{X\,max,NMA\beta a} \quad (19)$$

The H_X nucleus was used to calculate logk^{α}_{N}, by fitting Eq. (17) to $\Delta\delta_{(pH)X}$ and [H$^+$] experimental data pairs, resulting in logk^{α}_{N} =

Table 3
Maximum protonation shifts of carbon-bound hydrogens in NMA and its two monoamide derivatives, and normalized C constants of NMA, for the α- and β-carboxylates

Nucleus	$\Delta\delta_{(pH)max}$ (ppm)			Sum of NMAαa and NMAβa $\Delta\delta_{(pH)max}$ values	Normalized C constants of NMA	
	NMA	NMAαa	NMAβa		C_α	C_β
H_X	0.580	0.154	0.423	0.154 + 0.423 = 0.577	0.425	0.154
H_A	0.430	0.381	0.163	0.381 + 0.163 = 0.544	0.301	0.129
H_B	0.504	0.397	0.187	0.397 + 0.187 = 0.584	0.342	0.162

Table 4
The macroscopic and microscopic protonation constants of NMA in log units

Macroconstants		Microconstants					
Symbol	Value	Symbol	Value	Symbol	Value	Symbol	Value
K_1	10.06	k^{N}	10.06	k^{β}	4.56	k^{α}	4.34
K_2	3.54	k^{N}_{β}	9.01	k^{β}_{N}	3.51	k^{α}_{N}	2.35
K_3	1.85	k^{N}_{α}	8.07	k^{β}_{α}	4.09	k^{α}_{β}	3.87
		$k^{N}_{\beta,\alpha}$	7.02	$k^{\beta}_{N,\alpha}$	3.04	$k^{\alpha}_{N,\beta}$	1.88

Site of protonation methylamino β-carboxylate α-carboxylate.

2.29, which provides a similarly good agreement in the other constants ($\log k^{\beta}_{N} = 3.51$, $\log k^{\alpha}_{N,\beta} = 1.88$ and $\log k^{\beta}_{N,\alpha} = 3.10$).

Introducing interactivity parameter between α- and β-carboxylates in aspartic acid [29] ($pE^{\alpha\beta} = 0.39$) into Eq. (24), and combining Eqs. (10), (11) and (24) also allow the calculation of a set of microconstants as another control: $\log k^{\alpha}_{N} = 2.26$, $\log k^{\beta}_{N} = 3.52$, $\log k^{\alpha}_{N,\beta} = 1.87$ and $\log k^{\beta}_{N,\alpha} = 3.13$.

7. Elucidation of the NMA microconstants for the minor protonation pathways

Taking into account the $\log K_1 = 10.06$, $\log K_2 = 3.54$ and $\log K_3 = 1.85$ macroconstants, and the $\log k^{\beta}_{N} = 3.51$, $\log k^{N}_{\alpha} = 2.35$, $\log k^{\alpha}_{N,\beta} = 1.88$ and $\log k^{N}_{\alpha,\beta} = 3.04$ microconstants of NMA, accepting $\log K_1 = \log k^{N}$, $\log K_{1NMA\beta a} = \log k^{N}_{\beta}$, $\log K_{1NMA\alpha a} = \log k^{N}_{\alpha}$, $\log K_{1NMA\alpha\beta a} = \log k^{N}_{\beta,\alpha}$ as well, and using Eqs. (7)–(9), all the remaining NMA microconstants could be calculated as follows (Eqs. (20)–(23)):

$$\log k^{\alpha} = \log K_1 K_2 K_3 - \log k^{N}_{\alpha} - \log k^{\beta}_{N,\alpha} \quad (20)$$

$$\log k^{\beta}_{\alpha} = \log K_1 K_2 K_3 - \log k^{\alpha} - \log k^{N}_{\alpha,\beta} \quad (21)$$

$$\log k^{\beta} = \log K_1 K_2 K_3 - \log k^{N}_{\beta} - \log k^{\alpha}_{N,\beta} \quad (22)$$

$$\log k^{\alpha}_{\beta} = \log K_1 K_2 K_3 - \log k^{\beta} - \log k^{N}_{\beta,\alpha} \quad (23)$$

All NMA macro- and microconstants are collected in Table 4. Since microconstants are to be necessarily derived from at least two sources, their ambiguity exceeds that of the macroconstants. Estimated ambiguities in the microconstants are 0.05–0.15 log units, except for k^{N}, where standard deviation holds, and k^{β}_{N} and $k^{\alpha}_{N,\beta}$, where those are less than 0.1 log units.

8. Interpretation of the site-specific basicities

Basicity of the NMA methylamino group is approximately 0.5 log units greater than the amino group basicity of aspartic acid. Such difference is well-known for primary and secondary amines. A less trivial question is how the inductive effects of amino and methylamino groups influence the basicity of carboxylates. Both α- and β-carboxyl groups proved to be more acidic in NMA than in aspartic acid. This result is in accordance with the acid-strengthening effects of protonated amino groups reported in the comprehensive work of Perrin et al. [37], who reported 2.43, 2.81 and 2.93 pK_a unit drops in the carboxylate basicity upon exchanging a carbon-bound hydrogen in α-position for $-NH_3^+$, $-NH(CH_3)_2^+$ and $-N(CH_3)_3^+$ moiety, respectively. The monotonic tendency of increasing $-\Delta pK_a$ values along the increment of methyl substituents shows the enhanced electron-withdrawing effects of ammonium groups. This observation is particularly interesting in view of the fact that the observed amino protonation constants are the largest ones for the secondary amines, supporting the hypothesis that amino electron densities increase monotonously in the primary < secondary < tertiary order, but protonation is practically hampered in the case of tertiary amines.

The NMA microconstant values quantitate that the α-carboxylate is about 15 times less basic than its β-counterpart, due to closer proximity and the inductive effect of the protonated methylamino moiety. Concomitantly, the pH-independent concentration ratio of microspecies $NMA_{N\beta}$ and $NMA_{N\alpha}$ can be calculated as $[NMA_{N\beta}]/[NMA_{N\alpha}] = k^{\beta}_{N}/k^{\alpha}_{N} = 14.45$. Note that these values are pH-independent ones, but they do depend on ionic strength, temperature and medium. In contrast, pair interactivity parameters are robust ones, they largely retain their values under different circumstances. Pair interactivity parameters (E, $\log E$) quantitate the effect of protonation at one site on the basicity of the other site and vice versa. Their values are usually expressed in log units:

$$\log E_{\alpha-\beta} = \log k^{\alpha} - \log k^{\alpha}_{\beta} = \log k^{\beta} - \log k^{\beta}_{\alpha} \quad (24)$$

$$\log E_{N-\alpha} = \log k^{\alpha} - \log k^{\alpha}_{N} = \log k^{N} - \log k^{N}_{\alpha} \quad (25)$$

$$\log E_{N-\beta} = \log k^{\beta} - \log k^{\beta}_{N} = \log k^{N} - \log k^{N}_{\beta} \quad (26)$$

The actual values for NMA are as follows: $\log E_{\alpha-\beta} = 0.47$, $\log E_{N-\alpha} = 1.99$ and $\log E_{N-\beta} = 1.05$. Comparing the latter two values to amino basicities of the parent NMA and its α-, β- and diamides (10.06, 8.07, 9.01 and 7.02, respectively) strikingly perfect additivity is observed.

Mole fraction of a certain species (f) can be expressed in terms of hydrogen ion concentration and protonation constants. For instance $f_{NMA_{N\alpha}}$ can be calculated at any pH as it is given by Eq. (27) (C_T is the total concentration of all NMA species).

$$f_{NMA_{N\alpha}} = \frac{[NMA_{N\alpha}]}{C_T} = \frac{k^{N}k^{\alpha}_{N}[H^+]^2}{1 + K_1[H^+] + K_1K_2[H^+]^2 + K_1K_2K_3[H^+]^3} \quad (27)$$

Mole fractions of all possible species can be depicted as a function of pH in the microspeciation curve. Fig. 3 shows that microspecies $NMA_{N\beta}$ dominates over $NMA_{N\alpha}$ at any pH, so the major pathway of protonation includes the species NMA, NMA_N $NMA_{N\beta}$ and $NMA_{N\alpha\beta}$.

Fig. 4 shows the complete distribution diagram of all the eight NMA microspecies. Parallel running lines refer to protonation isomers. Some of them (for example, NMA_α NMA_β and $NMA_{\alpha\beta}$) are inferiorly minor species, occurring in concentration orders of magnitude below their major protonation isomer counterparts.

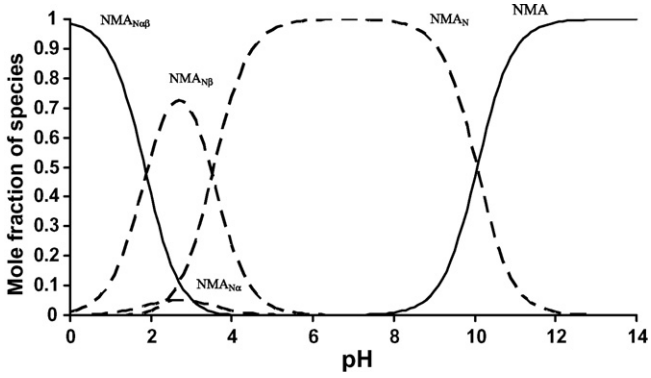

Fig. 3. Distribution curves of the five most abundant species of NMA as a function of pH: (A) NMA, (B) NMA_N, (C) $NMA_{N\beta}$, (D) $NMA_{N\alpha}$ and (E) $NMA_{N\alpha\beta}$.

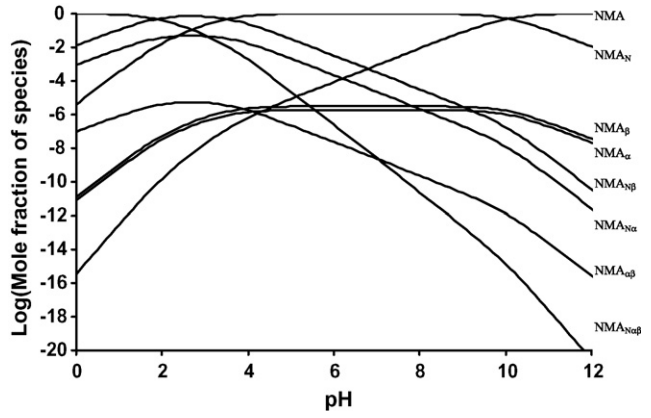

Fig. 4. Logarithmic distribution curves of all possible species of NMA as a function of pH: (A) NMA, (B) NMA_N, (C) NMA_β, (D) NMA_α, (E) $NMA_{N\beta}$, (F) $NMA_{N\alpha}$, (G) $NMA_{\alpha\beta}$ and (H) $NMA_{N\alpha\beta}$.

9. Conclusions

The complete microspeciation reveals the concentration of every microspecies, including the minor ones. In biochemical processes the highly specific circumstances may promote the minor species to be the reactive ones [38]. This statement can especially be true for NMA, which acts in the central nervous system, where the lipoic medium and the concomitant low dielectric constant elevate the carboxylate basicities by orders of magnitude, and leaves the amino basicity at the aqueous level [39]. In particular, $NMA_{\beta\alpha}$ the only chargeless species is typically of low concentration at any pH, nevertheless, it may actually be the best complying one in the lipoid bilayer of cell membranes and the characteristically lipoid brain areas. The species-specific NMR and distribution data of NMA allow selective analytical determinations under various circumstances.

Furthermore, the electrostatic interactions are of great importance in biological media in processes of molecular recognition, especially in receptor–ligand binding. In the field of designing NMDA agonists and antagonists, the steric and electronic features governing the selectivity of binding have recently been reported [8,16]. The lack of submolecular physicochemical data, however, precluded the thermodynamic quantitation of NMDA receptor binding. Complete determination of microscopic protonation constants of NMA species provides fundamental physicochemical data to improve and develop highly predictive receptor-binding operational models [40] of NMDA receptors, and also, to design new therapeutic agents with improved potency, selectivity and pharmacokinetic properties.

Acknowledgements

This work was supported by OTKA T 04359 and ETT 535/03 fundings. The authors thank Dr. Zoltan Szakacs for contribution in the evaluation of pH-potentiometric titration data.

References

[1] P. Wahl, U. Madsen, T. Banke, P. Krogsgaard-Larsen, A. Schousboe, Eur. J. Pharmacol. 308 (1996) 211–218.
[2] J.R. Greenwood, H.R. Capper, R.D. Allan, G.A.R. Johnston, Internet J. Chem. 1 (1998) 38.
[3] A. Seleni, S. D'Aniello, A.F. Perna, D. Ingrosso, Faseb J. 14 (2000) 699–714.
[4] T.W. Robbins, E.R. Murphy, Trends Pharmacol. Sci. 27 (2006) 141–148.
[5] D. Catarzi, V. Colotta, F. Varano, Curr. Top. Med. Chem. 6 (2006) 809–821.
[6] H.S.V. Chen, S.A. Lipton, J. Neurochem. 97 (2006) 1611–1626.
[7] K.R. Gogas, Curr. Opin. Pharmacol. 6 (2006) 68–74.
[8] A.M. Gerber, M.L. Vallano, Mini-Rev. Med. Chem. 6 (2006) 805–815.
[9] C.W. Lindsley, W.D. Shipe, S.E. Wolkenberg, C.R. Theberge, D.L. Williams, C. Sur, G.G. Kinney, Curr. Top. Med. Chem. 6 (2006) 771–785.
[10] Tuominen H.J., Tiihonen J., Wahlbeck K., Glutamatergic drugs for schizophrenia (Cochrane Review), The Cochrane Database of Systematic Reviews, 2006, Issue 2, Art. No.: CD003730. doi:10.1002/14651858.CD003730.
[11] A.J. Robichaud, Curr. Top. Med. Chem. 6 (2006) 553–568.
[12] M. Kraszni, J. Kokosi, B. Noszal, J. Chem. Soc., Perkin Trans 2 (2002) 914–917.
[13] M. Kraszni, Z. Szakács, B. Noszál, Anal. Bioanal. Chem. 378 (2004) 1449–1463.
[14] Z. Szakács, M. Kraszni, B. Noszál, Anal. Bioanal. Chem. 378 (2004) 1428–1448.
[15] U. Madsen, H. Brauner-Osborne, J.R. Greenwood, T.N. Johansen, P. Krogsgaard-Larsen, T. Liljefors, M. Nielsen, B. Frolund, in: Gad S.C. (Ed.), Drug Discovery Handbook, John Wiley & Sons Ltd., Chichester West Sussex, 2005, pp. 797–907 (Chapter 18).
[16] P.E. Chen, D.J.A. Wyllie, Br. J. Pharmacol. 147 (2006) 839–853.
[17] H.M. Irving, M.G. Miles, L.D. Pettit, Anal. Chim. Acta 38 (1967) 475–488.
[18] D.J. Leggett (Ed.), Computational Methods for the Determination of Formation Constants, Plenum Press, New York, 1986.
[19] B. Noszál, Z. Szakács, J. Phys. Chem. B 107 (2003) 5074–5080.
[20] Z. Szakács, G. Hagele, R. Tyka, Anal. Chim. Acta 522 (2004) 247–258.
[21] S. Sjöberg, Pure Appl. Chem. 69 (1997) 1549–1570.
[22] A. Koeberg-Telder, H. Cerfontain, J. Chem. Soc., Perkin Trans. 2 (1975) 226–229.
[23] STATISTICA (Data Analysis Software System), Version 6, StatSoft Inc., 2001, http://www.statsoft.com/.
[24] http://www.Originlab.com/.
[25] E. Grunwald, A. Loewenstein, S. Meiboom, J. Chem. Phys. 27 (1957) 641–642.
[26] H. Günther, NMR Spectroscopy, John Wiley & Sons, Chinchester, 1980, pp. 151–170.
[27] R.G. Bates, Determination of pH, Theory and Practice, second ed., Wiley-Interscience, New York, NY, 1973.

[28] B. Noszál, in: K. Burger (Ed.), Biocoordination Chemistry: Coordination Equilibria in Biologically Active Systems, Ellis Horwood, Chichester, 1990, pp. 18–55 (Chapter 2).
[29] B. Noszál, P. Sándor, Anal. Chem. 61 (1989) 2631–6237.
[30] L. Ebert, Z. Phys. Chem. 121 (1926) 385–400.
[31] J.L. Sudmeier, C.N. Reilly, Anal. Chem. 36 (1964) 1698–1706.
[32] R.F. Jameson, G. Hunter, T.A. Kiss, J. Chem. Soc., Perkin Trans. 2 (1980) 1105–1110.
[33] T. Kiss, B. Tóth, Talanta 29 (1982) 539–544.
[34] E. Farkas, T. Kiss, B. Kurzak, J. Chem. Soc., Perkin Trans. 2 (1990) 1255–1257.
[35] H.L. Surprenant, J.E. Sarneski, R.R. Key, J.T. Byrd, C.N. Reilly, J. Magn. Reson. 40 (1980) 231–243.
[36] B. Noszál, W. Guo, D.L. Rabenstein, J. Org. Chem. 57 (1992) 2327–2334.
[37] D.D. Perrin, B. Dempsey, E.P. Serjeant, pK_a Prediction for Organic Acids and Bases, Chapman and Hall, London, 1981.
[38] Z. Szakacs, B. Noszal, Electrophoresis 27 (2006) 3399–3409.
[39] J. Nyiri, B. Noszal, J. Sol. Chem. 34 (2005) 1227–1233.
[40] M. Corsi, P. Fina, D.G. Trist, Trends Pharmacol. Sci. 17 (1996) 220–222.